Materials Science and Engineering A 527 (2010) 4191–4196

Contents lists available at ScienceDirect

Materials Science and Engineering A

journal homepage: www.elsevier.com/locate/msea

Investigation of superplasticity in friction stir processed 2219Al alloy

F.C. Liu, B.L. Xiao, K. Wang, Z.Y. Ma*

Shenyang National Laboratory for Materials Science, Institute of Metal Research, Chinese Academy of Sciences, 72 Wenhua Road, Shenyang 110016, China

ARTICLE INFO

Article history:
Received 7 January 2010
Received in revised form 7 March 2010
Accepted 16 March 2010

Keywords:
Superplasticity
Aluminum alloy
Friction stir processing
Grain growth

ABSTRACT

Commercial 2219Al–T6 alloy plates were friction stir processed (FSPed) at a rotation rate of 400 rpm and a traverse speed of 100 mm/min in water and air, producing two fine-grained 2219Al samples with average grain sizes of 1.0 and 2.1 μm, respectively. The 1.0 and 2.1 μm-2219Al retained fine-grained microstructure during annealing treatment at temperatures up to 400 and 425 °C, respectively, above which abnormal grain growth occurred. Superplasticity was observed in 1.0 μm-2219Al within the medium temperature range of 350–425 °C and a maximum ductility of 450% was obtained at 400 °C and 3×10^{-4} s^{-1}. Increasing the grain size from 1.0 to 2.1 μm resulted in a slight increase in the thermal stability, but did not enhance the superplasticity of the FSP 2219Al. The relatively low superplasticity in the FSP fine-grained 2219Al was attributed to unstable grain structure because the pining Al_2Cu particles were easily coarsened at high temperatures.

1. Introduction

Superplasticity of aluminum alloys has a great potential to provide an efficient near-net shape forming method for automobile components, aircraft skin and structural component in aerospace, since superplasticity is usually associated with a lower flow stress than most hot working conditions and total elongations of >200%. In the past few years, researchers developed a series of new superplastic alloys which exhibited excellent mechanical properties at room-temperature in addition to their high-temperature superplastic formability. An example of the new superplastic alloys is the Al–Cu–Zr alloys [1–4], in which fine grains are stabilized by Al_3Zr dispersoids. However, the processing of fine-grained Al–Cu–Zr alloys involves rapid chilling from the melt containing supersaturated Zr solutes, and then warm and cold working. This processing route is complicated and the size of fine-grained material that can be produced is limited, which restricts broader application of these alloys [5]. If superplasticity can be achieved in existing commercial alloys via simple processing routes, the applications of superplastic forming as a fabricating method will be widened.

For these reasons, there have been considerable research interests in developing superplasticity in commercial aluminum alloys, such as high-strength 2XXX series Al alloys. Among the 2XXX series aluminum alloys, 2219Al is widely used in the aerospace industry. Therefore, developing superplasticity in 2219Al is of practical importance. However, studies on the superplasticity of 2219Al are rather limited. Kaibyshev et al. [5] developed a fine-grained 2219Al with an average grain size of 12 μm via a two-step thermomechanical processing (TMP). The maximum superplastic elongation of 675% was recorded at 500 °C and a strain rate of 2.2×10^{-4} s^{-1}. Han and Langdon [6] produced an ultrafine-grained 2219Al with an average size of about 0.2 μm by equal-channel angular pressing (ECAP). However, the ultrafine-grained 2219Al did not exhibit superplasticity due to extensive grain growth at temperatures from 200 to 300 °C.

Friction stir processing (FSP) which was developed from friction stir welding (FSW) [7,8] has been demonstrated to be a potential grain refinement technique [9–11]. FSP results in the generation of fine recrystallized grains with predominant high-angle grain boundaries, which is critical for enhanced superplastic properties. This attracted many researchers to investigate superplastic behavior of FSP aluminum alloys. A number of aluminum alloys, such as 7075Al, 2024Al, 5083Al, A356, Al–Mg–Zr, Al–Mg–Sc, and Al–Zn–Mg–Sc, have been subjected to FSP and superplasticity investigations [10–22]. Excellent superplasticity has been obtained at high strain rates or low temperatures [10,15–22].

However, to the best of our knowledge, no study on superplasticity of FSP 2219Al has been reported so far. It is very interesting to demonstrate whether superplasticity can be obtained in 2219Al via FSP. In this study, we produced two fine-grained 2219Al alloys via FSP and examined the relationship of the microstructure and the superplasticity.

2. Experimental

A 6 mm thick 2219Al-T6 plate with a nominal composition of 6.27Cu, 0.28Mn, 0.21Fe, 0.14Zr, 0.24Si, 0.05Ti, and 0.08Zn (in wt.%) was used. FSP was preformed at a rotation rate of 400 rpm and a

* Corresponding author. Tel.: +86 24 83978908; fax: +86 24 83978908.
E-mail address: zyma@imr.ac.cn (Z.Y. Ma).

0921-5093/$ – see front matter © 2010 Elsevier B.V. All rights reserved.
doi:10.1016/j.msea.2010.03.065

traverse speed of 25 mm/min under air and water cooling conditions, respectively. The total FSP length was around 360 mm from pin entry to pin exit. The tool was manufactured from M42 steel with a concave shoulder 14 mm in diameter and a threaded conical pin 5 mm in root diameter and 3.5 mm in tip diameter, and 4.5 mm in length. Microstructure characterization was performed by scanning electron microscopy (SEM) and transmission electron microscopy (TEM). Thin foils for TEM were prepared by twin-jet polishing using a solution of 70% methanol and 30% nitric acid at −30 °C and 19 V.

To evaluate the superplastic behavior of FSP 2219Al, dog-bone shaped tensile specimens (2.5 mm gage length, 1.4 mm gage width and 1.0 mm gage thickness) were electro-discharge machined in the transverse direction. The gage length was centered in the stir zone (SZ). These specimens were subsequently ground and polished to a final thickness of ~0.8 mm. Constant crosshead speed tensile tests were conducted using INSTRON 5848 micro-tester. Each specimen was fastened in the tensile testing apparatus when the furnace was heated to the selected testing temperature. All specimens were held at the selected testing temperature for 20 min to establish thermal equilibrium prior to tensile test. The fractured specimens were subjected to SEM examinations.

To check the thermal stability of the fine grains produced by FSP, small specimens with a dimension of 6 mm × 6 mm × 10 mm cut from the FSP sample were statically annealed for 1 h at temperatures ranging from 200 to 475 °C, and then water quenched to provide microstructure information of the FSP samples at various temperatures.

3. Results and discussion

The as-received material was characterized by a typical hot-rolled structure, consisting of large elongated pancake shaped grains of several tens of micrometers length (Fig. 1a). Fig. 1b and c shows the TEM microstructure of the FSP 2219Al samples. The average grain sizes were estimated to be 1.0 and 2.1 μm for the FSP samples prepared in water and air, respectively. The small particles in the FSP samples were the Al_2Cu particles which were coarsened during FSP. It is noted that the Al_2Cu particles in the FSP sample prepared under water cooling condition were much smaller than that under air cooling condition.

Microstructure evolution during FSW/FSP has been widely investigated in the previous studies [8,10,16,18,23–25]. Intense plastic deformation and frictional heating during FSW/FSP resulted in the generation of a recrystallized fine-grained structure within the SZ [8]. It was reported that the initial size of newly recrystallized grains was in the range of 25–100 nm and grew to 2–5 μm, equivalent to that found in FSP aluminum alloys, after being heated for 1–4 min at 350–450 °C [25]. Therefore, if effective cooling is used to decrease the process temperature, a fine-grained structure can be obtained due to the prohibition of the growth of recrystallized grains. Thus, a finer grain size of ~1 μm was produced via FSP under water cooling condition. In comparison, FSP in air produced a larger grain size of ~2.1 μm in the SZ. Furthermore, FSP in air produced larger Al_2Cu particles due to a higher process temperature.

In a previous study [16], an ultrafine grain size of 0.6 μm was produced in an FSP Al–Mg–Sc alloy by using the same tool design and FSP parameters under water cooling condition as in the present study. In the Al–Mg–Sc alloy, a significant amount of thermally stable Al_3Sc particles could pin the grain boundaries effectively. Thus, the growth of recrystallized grains in the Al–Mg–Sc alloy was retarded during FSP. However, for the 2219Al alloy, the Al_2Cu particles in the SZ during FSP were easily coarsened, and therefore exhibited a lower pining force on the grain growth than the Al_3Sc particles, so relatively larger grains were obtained in the FSP 2219Al.

Fig. 2 shows the grain microstructure of the FSP 2219Al of 1.0 μm grain size (hereafter referred to as 1.0 μm-2219Al) after static annealing for 1 h at various temperatures. The 1.0 μm-2219Al exhibited excellent thermal stability during static annealing at 200 °C and the grain size was 1.1 μm (Fig. 2a). As the static annealing temperature increased, there was only a minor grain growth up to a temperature of ~400 °C. For example, the grains in the 1.0 μm-2219Al annealed at 375 and 400 °C for 1 h were 1.9 and 2.4 μm, respectively (Fig. 2b and c). With a further increase of the annealing temperature to 425 °C, abnormal grain growth (AGG) was observed in the 1.0 μm-2219Al (Fig. 2d). Furthermore, it is noted that with the increase of the annealing temperature, the density of the Al_2Cu

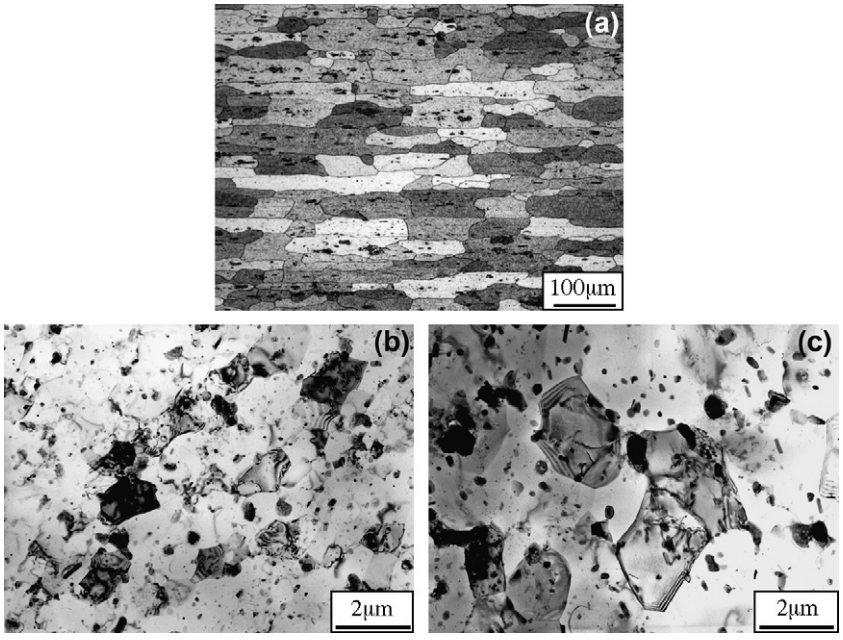

Fig. 1. Optical micrograph showing large elongated grains in (a) rolled 2219Al and TEM images showing fine and equiaxed grains in FSP 2219Al prepared in (b) water and (c) air.

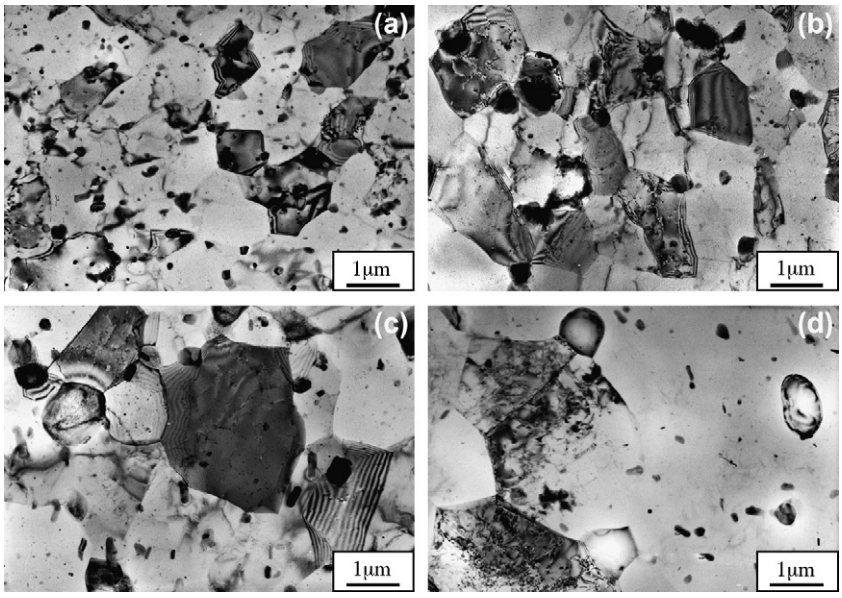

Fig. 2. Typical microstructure of 1.0 μm-2219Al after being annealed for 1 h at (a) 200 °C, (b) 375 °C, (c) 400 °C, and (d) 425 °C.

precipitates was significantly reduced, thereby reducing the pining effect on the grain growth. Similar phenomena were also observed in the annealed 2.1 μm-2219Al. Fig. 3 shows the variation of the grain size with the annealing temperature for the two FSP 2219Al samples. The 1.0 μm-2219Al retained grain sizes of <2.4 μm up to 400 °C, above which the AGG occurred. By comparison, the grains of the 2.1 μm-2219Al were relatively stable up to 425 °C.

Despite a number of microstructural studies on FSP aluminum alloys, fundamental understanding of the microstructural evolution during heat treatment is still poor. Charit and Mishra [26] suggested that the AGG in friction stirred materials was mainly associated with the inhomogeneous deformation pattern during the friction stir process. Ferry et al. [27] found that $dR/dt \propto dr/dt$ in the fine-grained Al–Sc alloy (R and r denote the radiuses of the grains and the particles, respectively, and t is the annealing time). This indicated that grain coarsening was controlled by the rate of particle growth. Hassan et al. [28] showed that the instability of the SZ grain structure was highly dependent on the welding parameters for FSP 7010Al. Low heat input resulted in an exceptionally fine and unstable grain structure in the SZ. The AGG occurred throughout the SZ during solution treatment, promoted by the dissolution of soluble precipitates. This is in good agreement with a unified theory of the stability of cellular microstructure, proposed by Humphreys [29]. When the welds were produced with higher inputs, the SZ grain structure was more stable during solution treatment, as the grain structure was coarser relative to the dispersoid density.

The present experimental results are consistent with the above observations. The unstability of the fine-grained structure in the FSP 2219Al is mainly attributed to the coarsening and dissolution of the Al_2Cu precipitates. FSP with water cooling (low heat input) produced 1 μm grain structure in 2219Al. There was only a minor grain growth when the samples were annealed at temperatures ≤400 °C. With a further increase in the annealing temperature, AGG was observed in the 1.0 μm-2219Al due to the dissolution of the fine Al_2Cu precipitates. On the other hand, the 2.1 μm-2219Al prepared in air (high heat input) was more stable due to its large initial grain structure.

Fig. 4 shows the true stress–true strain (σ–ε) curves for the 1.0 μm-2219Al deformed at $3 \times 10^{-4}\,s^{-1}$ and at various temperatures. The curves show continuous strain hardening up to substantial strain values. Such curves are typical of materials undergoing concurrent grain coarsening [30].

Fig. 5a shows the variation of elongation of the 1.0 μm-2219Al as a function of the initial strain rate at 400 °C. Superplastic ductility was achieved over a wide strain rate range of 1×10^{-4} to $1 \times 10^{-2}\,s^{-1}$ and a maximum ductility of 450% was obtained at 400 °C and $3 \times 10^{-4}\,s^{-1}$. The variation of elongation with the initial strain rate for the 2.1 μm-2219Al is shown in Fig. 5b. The maximum ductility of 400% was obtained at 425 °C and $3 \times 10^{-4}\,s^{-1}$. In contrast to the 12 μm-2219Al prepared by TMP [5], in which the maximum elongation of 675% was obtained at 500 °C and a strain rate of $2.2 \times 10^{-4}\,s^{-1}$, the two FSP 2219Al exhibited lower

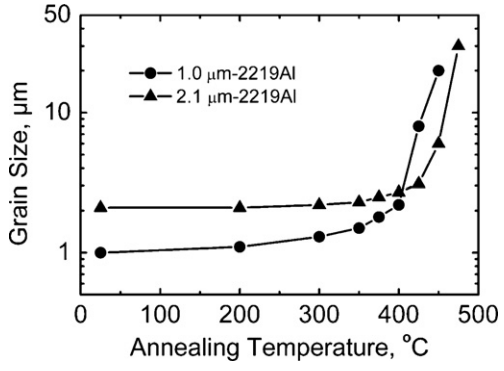

Fig. 3. Variation of grain size with annealing temperature for FSP 2219Al.

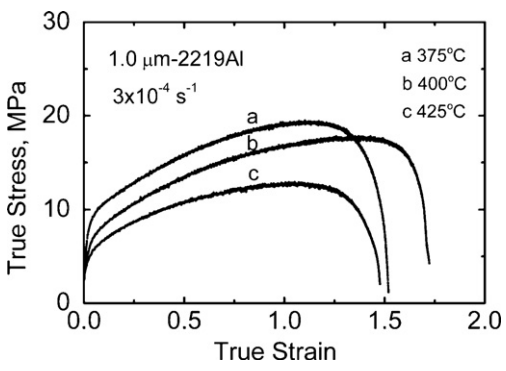

Fig. 4. True stress–strain curves of 1.0 μm-2219Al deformed at $3 \times 10^{-4}\,s^{-1}$.

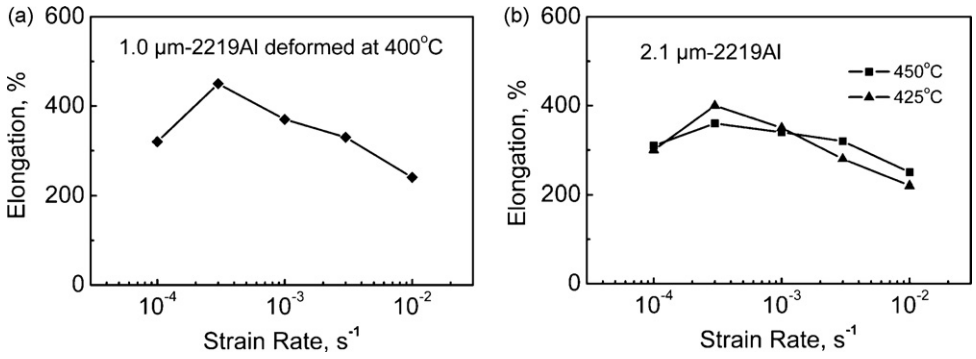

Fig. 5. Variation of ductility with initial strain rate for (a) 1.0 μm-2219Al and (b) 2.1 μm-2219Al.

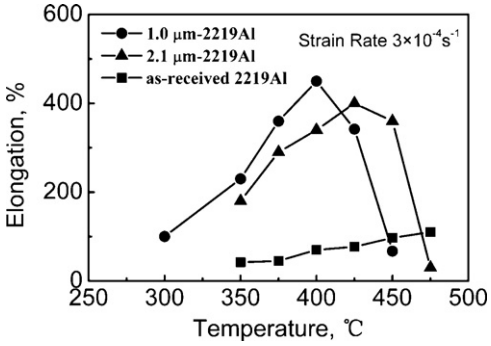

Fig. 6. Variation of elongation with test temperature at an initial strain rate of $3 \times 10^{-4}\ s^{-1}$ for rolled 2219 Al, and 1.0 and 2.1 μm-2219Al.

superplastic elongations. However, the optimum superplasticity temperature was significantly reduced for the FSP 2219Al.

Fig. 6 shows the effect of temperature on the superplastic ductility of the rolled and FSP 2219Al at $3 \times 10^{-4}\ s^{-1}$. At temperatures of 350–475 °C, the elongations of less than 120% were observed in the rolled sample, indicating that no superplasticity was obtained. Compared to the rolled sample, the FSP samples exhibited a significant enhanced superplasticity. Ductility of the 1.0 μm-2219Al increased with an increase of the testing temperature until 400 °C, and then decreased rapidly with increasing the temperature. The 2.1 μm-2219Al exhibited a shift of optimum superplasticity temperature to a higher value. This corresponds well with the result that the 2.1 μm-2219Al showed a better thermal stability (Fig. 3).

Fig. 7 shows the grain growth in the 1.0 μm-2219Al specimens deformed to failure at 425 and 450 °C. For 425 °C, the gage of the tensile specimen exhibited a duplex microstructure with a small number of large grains being surrounded by arrays of fine grains (Fig. 7b and c). This indicates that AGG occurred at 425 °C during superplastic tension, resulting in the decrease in superplastic elongation. At 450 °C, the grains in the gage grew to several hundred micrometers (Fig. 7a), leading to the disappearance of superplasticity. Therefore, rapid decrease in ductility of the 1.0 μm-2219Al with the temperature at temperatures higher than 400 °C is attributed to the occurrence of AGG during superplastic deformation.

The flow stress taken at a true strain of 0.1 is plotted as a function of the initial strain rate on the double logarithmic scales in Fig. 8a and b. The strain rate sensitivity (m value) of the 1.0 and 2.1 μm-2219Al ranged from 0.3 to 0.4 in the superplastic range. This value is lower than 0.5, a typical value for superplastic deformation dominated by grain boundary sliding (GBS). The relatively low m values may imply that besides GBS, other deformation processes such as dislocation or diffusion accommodation were also operative during the superplastic deformation of the FSP 2219Al.

Fig. 9a–c shows the distribution of second-phase particles in the base metal (BM), as-FSP sample and the deformed sample. In the 2219Al-T6 BM, a few large second-phase particles θ (Al_2Cu)

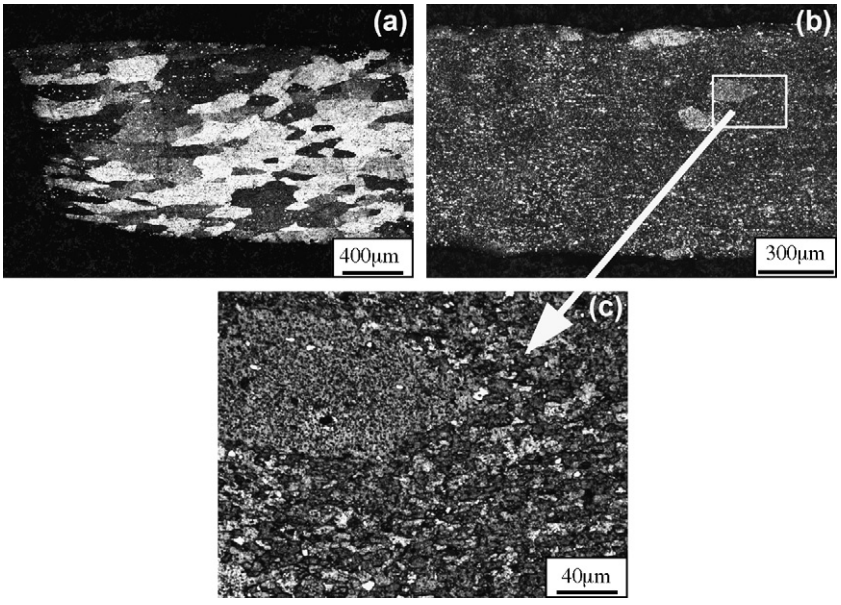

Fig. 7. Optical micrographs showing grain growth in the gage of 1.0 μm-2219Al specimens deformed to failure at (a) 450 °C, (b) and (c) 425 °C at $3 \times 10^{-4}\ s^{-1}$.

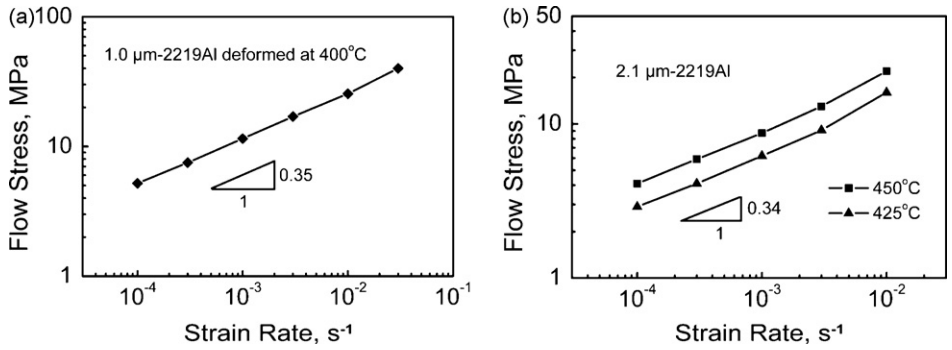

Fig. 8. Variation of flow stress with initial strain rate for (a) 1.0 μm-2219Al and (b) 2.1 μm-2219Al.

were observed and the very fine metastable precipitates were not discernible under SEM. The 1.0 μm-2219Al was characterized by some large particles and a great amount of small particles. Chen et al. [31] reported that high-temperature forced relatively large metastable precipitates overage to the equilibrium phases, whereas relatively small metastable precipitates dissolved during friction stir welding of 2219-T6 aluminum alloy. In this study, the small particles in the FSP 2219Al should come from the coarsening of fine metastable precipitates as well as the breakup of large particles. During high-temperature superplastic deformation, the small precipitates in the FSP sample were significantly coarsened (Fig. 9c). This is a direct reason for the rapid grain growth in the FSP 2219Al during superplastic deformation at higher temperatures (Fig. 7).

In this study, we produced two fine-grained 2219Al with the grain sizes of 1.0 and 2.1 μm, respectively. The FSP 2219Al exhibited a maximum elongation of 450% at 400 °C and $3 \times 10^{-4}\ s^{-1}$, which was lower than that of the Al–Cu–Zr alloys with a Zr content of 0.4–0.5 wt.% [1–4]. The Al–Cu–Zr alloys demonstrate excellent superplastic properties (800–1200% at 480 °C and $1 \times 10^{-3}\ s^{-1}$) due to the presence of numerous Al_3Zr particles which can effectively prohibit the grain growth during superplastic deformation. The 2219Al has a higher Cu content (6.27 wt.%) and a lower Zr content (0.14 wt.%). The main pining particles in the 2219Al are Al_2Cu particles. The Al_2Cu particles are not as thermally stable as the Al_3Zr particles [32] and easily coarsened at high temperatures. In this case, they cannot effectively inhibit the grain growth during superplastic deformation.

Reducing grain size was usually beneficial to enhancing superplasticity [20–23,33–37]. However, the thermal stability of the fine-grained materials decreases with the decrease of the grain size. For the aluminum alloys with a great amount of thermally stable particles such as Al_3Zr or Al_3Sc, excellent high strain rate/low-temperature superplasticity could be obtained in the fine-grained structure due to good thermal stability of the fine-grained structure resulting from effective pining of these particles [16–19,21]. If the pining particles in the aluminum alloys are not thermally stable, it is difficult to obtain good superplasticity due to extensive growth of the fine grains at high temperatures. In the 12 μm-2219Al produced by TMP, Kaibyshev et al. [5] obtained a superplasticity of 675% at 500 °C and $2.2 \times 10^{-4}\ s^{-1}$. This superplasticity is much

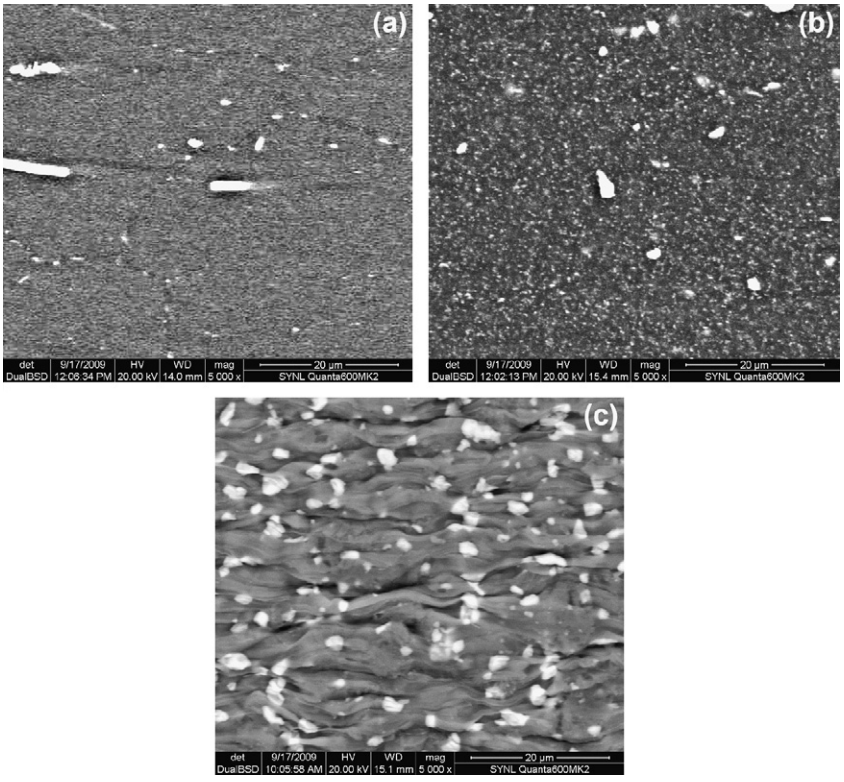

Fig. 9. Backscattered electron images of (a) base metal, (b) 1.0 μm-2219Al, and (c) 1.0 μm-2219Al deformed at 400 °C and $3 \times 10^{-4}\ s^{-1}$.

lower than that obtained in the Al–Cu–Zr alloys [1–4]. Reducing the grain size to 0.2 μm in the 2219Al by ECAP [6], no superplasticity was achieved at temperatures from 200 to 300 °C due to the extensive grain growth. In this study, the 1.0 and 2.1 μm-2219Al showed a better thermal stability than the 0.2 μm-2219Al, and exhibited medium superplasticity within the medium temperature ranges of 350–425 and 375–450 °C, respectively. Increasing the grain size from 1.0 to 2.1 μm resulted in a slight increase in the thermal stability (Fig. 3), but did not enhance the superplasticity of the FSP 2219Al (Figs. 5 and 6). The elongation and optimum strain rate were relatively lower. With further increasing the test temperature, superplasticity disappeared in the FSP 2219Al because the AGG occurred. The AGG has been reported in several FSP/FSW aluminum alloys [16,19,38]. It might be associated with the high fraction of high-angle grain boundaries in the FSP/FSW aluminum alloys.

From Refs. [5,6] and the present study, it seems to be difficult to obtain a high elongation in the high strain rate range in the commercial 2219Al. Refining the grain size to too small scale is not a good strategy to enhance the superplasticity of the 2219Al due to poor thermal stability of the fine-grained 2219Al. However, it is possible to obtain medium superplasticity in the 2219Al with a medium grain size. In order to obtain excellent superplastic properties in the 2219Al, a certain amount of Zr or Sc element should be added to improve its thermal stability.

4. Conclusions

1. Fine-grained 2219Al alloys with a grain size of 1.0 and 2.1 μm were produced via FSP at 400 rpm and 100 mm/min in water and air, respectively. The fine metastable precipitates in the 2219Al-T6 were significantly coarsened.
2. The 1.0 and 2.1 μm-2219Al retained fine grain structure up to 400 and 425 °C, respectively. Above 400 and 425 °C, abnormal grain growth occurred in the two FSP samples.
3. The FSP 2219Al showed enhanced superplastic properties compared to the rolled 2219Al. The 1.0 and 2.1 μm-2219 Al exhibited a maximum ductility of 450% at 400 °C and 3×10^{-4} s^{-1} and 400% at 425 °C and 3×10^{-4} s^{-1}, respectively.
4. Relatively low superplasticity in the FSP fine-grained 2219Al was attributed to unstable grain structure because the pining Al_2Cu particles were easily coarsened at high temperatures.

Acknowledgments

This work was supported by the National Natural Science Foundation of China under grant Nos. 50671103 and 50871111, the National Basic Research Program of China under grant No. 2006CB605205, the National Outstanding Young Scientist Foundation under Grant No. 50525103, and the Hundred Talents Program of Chinese Academy of Sciences.

References

[1] B.M. Watts, M.J. Stowell, B.L. Baikie, D.G.E. Owen, Met. Sci. 10 (1976) 189–205.
[2] R. Grimes, M.J. Stowell, B.M. Watts, Met. Technol. 3 (1976) 154–160.
[3] R.H. Bricknell, J.W. Edington, Metall. Trans. A 10 (1979) 1257–1263.
[4] R.Z. Valiev, A.V. Korznikov, R.R. Mulyukov, Mater. Sci. Eng. A 168 (1993) 141–148.
[5] R. Kaibyshev, I. Kazakulov, D. Gromov, F. Musin, D.R. Lesuer, T.G. Nieh, Scripta Mater. 44 (2001) 2411–2417.
[6] B.Q. Han, T.G. Langdon, 2nd International Symposium on Ultrafine Grained Materials, Seattle, USA, February, 2002, pp. 485–494.
[7] W.M. Thomas, E.D. Nicholas, J.C. Needham, M.G. Murch, P. Templesmith, C.J. Dawes, G.B. Patent Application No. 9125978.8, December 1991.
[8] R.S. Mishra, Z.Y. Ma, Mater. Sci. Eng. R 50 (2005) 1–78.
[9] R.S. Mishra, M.W. Mahoney, S.X. McFadden, N.A. Mara, A.K. Mukherjee, Scripta Mater. 42 (2000) 163–168.
[10] Z.Y. Ma, R.S. Mishra, M.W. Mahoney, Acta Mater. 50 (2002) 4419–4430.
[11] Z.Y. Ma, R.S. Mishra, M.W. Mahoney, R. Grimes, Metall. Mater. Trans. A 36 (2005) 1447–1458.
[12] L.B. Johannes, I. Charit, R.S. Mishra, R. Verma, Mater. Sci. Eng. A 464 (2007) 351–357.
[13] Z.Y. Ma, R.S. Mishra, F.C. Liu, Mater. Sci. Eng. A 505 (2009) 70–78.
[14] Z.Y. Ma, R.S. Mishra, M.W. Mahohey, R. Grimes, Mater. Sci. Eng. A 351 (2003) 148–153.
[15] I. Charit, R.S. Mishra, Mater. Sci. Eng. A 359 (2003) 290–296.
[16] F.C. Liu, Z.Y. Ma, L.Q. Chen, Scripta Mater. 60 (2009) 968–971.
[17] F.C. Liu, Z.Y. Ma, Scripta Mater. 59 (2008) 882–885.
[18] F.C. Liu, Z.Y. Ma, Scripta Mater. 62 (2010) 125–128.
[19] I. Charit, R.S. Mishra, Acta Mater. 53 (2005) 4211–4223.
[20] Z.Y. Ma, R.S. Mishra, M.W. Mahoney, Scripta Mater. 50 (2004) 931–935.
[21] Z.Y. Ma, R.S. Mishra, Scripta Mater. 53 (2005) 75–80.
[22] F.C. Liu, Z.Y. Ma, Scripta Mater. 58 (2008) 667–670.
[23] I. Charit, R.S. Mishra, J. Mater. Res. 19 (2004) 3329–3342.
[24] J.Q. Su, T.W. Nelson, C.J. Sterling, Mater. Sci. Eng. A 405 (2005) 277–286.
[25] C.G. Rhodes, M.W. Mahoney, W.H. Bingel, M. Calabrese, Scripta Mater. 48 (2003) 1451–1455.
[26] I. Charit, R.S. Mishra, Scripta Mater. 58 (2008) 367–371.
[27] M. Ferry, N.E. Hamilton, F.J. Humphreyst, Acta Mater. 53 (2005) 1097–1109.
[28] Kh.A.A. Hassan, A.F. Norman, D.A. Price, P.B. Prangnell, Acta Mater. 51 (2003) 1923–1936.
[29] F.J. Humphreys, Acta Mater. 45 (1997) 5031–5039.
[30] R.S. Mishra, T.R. Bieler, A.K. Mukherjee, Acta Metall. Mater. 43 (1995) 877–891.
[31] Y.C. Chen, J.C. Feng, H.J. Liu, Mater. Charact. 60 (2009) 476–481.
[32] K.S. Kumar, S.A. Brown, J.R. Pickens, Acta Mater. 44 (1996) 1899–1915.
[33] Z. Horita, M. Furukawa, M. Nemoto, A.J. Barnes, T.G. Langdon, Acta Mater. 48 (2000) 3633–3640.
[34] F. Musin, R. Kaibyshev, Y. Motohashi, G. Itoh, Scripta Mater. 50 (2004) 511–516.
[35] S. Komura, Z. Horita, M. Furukawa, M. Nemoto, T.G. Langdon, Metall. Mater. Trans. A 32 (2001) 707–716.
[36] Z. Horita, T.G. Langdon, Scripta Mater. 58 (2008) 1029–1032.
[37] T.G. Nieh, L.M. Hsiung, J. Wadsworth, R. Kaibyshev, Acta Mater. 46 (1998) 2789–2800.
[38] M.M. Attallah, H.G. Salem, Mater. Sci. Eng. A 391 (2005) 51–59.